TARGET TRACKING THROUGH A COORDINATED TURN

Mark R. Morelande

CRC for Sensor, Signal and Information Processing
Department of Electrical and Electronic Engineering
The University of Melbourne, Australia
m.morelande@ee.mu.oz.au

Neil J. Gordon

Tracking and Sensor Fusion Group
DSTO, Australia
Neil.Gordon@dsto.defence.gov.au

ABSTRACT

Allowing for perturbations in speed and turn rate, the state of a target moving in a coordinated turn obeys a nonlinear stochastic differential equation which cannot be discretised exactly. Existing algorithms for coordinated turn tracking avoid this problem by ignoring perturbations in the continuous-time model and adding process noise only after discretisation. We retain this modelling by discretising using first and second order Taylor approximations to the continuous-time coordinated turn dynamic model. The discrete-time models are used as the basis for a particle filter for tracking a target moving in a coordinated turn. The performances of the discretisation techniques and the effect of different coordinate systems on tracking performance are examined.

1. INTRODUCTION

A coordinated turn (CT) commonly refers to a target manoeuvre executed under constant speed along a circular path at a constant altitude. This type of motion is common in civil aircraft. In such cases the horizontal motion and vertical motion of the target can be considered to be decoupled and therefore tracked separately. We restrict our attention to the horizontal motion of the aircraft as the vertical motion can be tracked separately using a simple linear/Gaussian model [2].

The aim of this paper is to develop suitable models to describe the horizonal motion of an object undergoing a CT and to propose and analyse algorithms for tracking the object. We begin with a continuous-time dynamic model to describe the evolution of the state of a target undergoing a coordinated turn. Although the CT model prescribes constant speed and constant turn rate this is an idealisation which is not met in practice. The dynamic model used here therefore adds small perturbations, modelled as independent Wiener processes, to the speed and turn rate. The target state is to be recursively estimated from noisy discrete-time measurements of the target's range and bearing.

Solution of the tracking problem requires recursive computation of the distribution of the target state conditional upon the measurement history. The necessary theory is readily available [8] but a closed-form solution for the posterior distribution cannot be obtained for the nonlinear dynamic and measurement equations used here. It is therefore necessary to resort to approximations.

The majority of filtering approximations, e.g., linearisation [8], the unscented transformation [9], debiasing [11] or particle filters [6], rely on the availability of a stochastic difference equation describing the evolution of the target state. In most target tracking applications such an equation can be readily derived from the continuous time dynamic equation. This is not so for the nonlinear dynamic equation used here. However, a stochastic difference equation which approximates the CT motion can be derived. In this paper we derive first and second order weak Taylor approximations [10]. Previous work on CT tracking has concentrated on discretisation of the drift function but has ignored the driving process [2, 7]. This is undesirable since the driving process of the continuous-time dynamic model is selected in order to model a certain characteristic of the target motion. In order to retain this modelling in the discrete-time approximation the driving process must also be discretised.

Given a stochastic difference equation for the target motion any number of methods can be used to approximate the posterior distribution. In this paper we propose a particle filtering algorithm [6]. Particle filters represent the posterior distribution of the target state by a set of random samples, or particles, with associated weights [1, 6]. Discretisation using the first order weak Taylor approximation has been suggested in the context of particle filtering in [5]. For m discretisation intervals per sampling interval and n particles, convergence of this scheme in m and n was proved under the condition that $m(n) \to \sqrt{n}$ as $n \to \infty$. It may be hypothesised that similiar convergence results could be obtained for the more accurate discretisation used in this paper.

An important issue in CT tracking is the effect of the coordinate system used in the target state on tracking accuracy. It was shown in [7] that, when using the EKF, better performance can be achieved if the target velocity is expressed as a magnitude and direction, i.e., polar velocity, instead of in the x and y directions, i.e., Cartesian velocity. Motivated by these results, the dependence of tracking performance on the velocity model will be investigated for the more realistic CT motion model used here.

Throughout this paper it is assumed that we begin tracking at the start of the turn with some prior distribution for the target state and finish tracking at the end of the turn. A practical tracking algorithm must also include mechansims for transitioning between the different modes of flight [2].

The paper is organised as follows. Section 2 contains the dynamic and measuremen models. Discretised approximations of the dynamic models are derived in Section 3 and used in the development of a particle filtering algorithm in Section 4. The performance of the tracking algorithm is analysed in Section 5. Conclusions are given in Section 6.

2. CT DYNAMIC AND MEASUREMENT MODELS

Stochastic differential equations (SDEs) describing the motion of an object undergoing a CT will be given for the polar velocity and Cartesian velocity models.

Work supported by DSTO under TDFL

2.1. Polar velocity dynamic model

For the polar velocity model, the state vector is taken as $x_t = (\xi_t, \zeta_t, s_t, \theta_t, \omega_t)'$ where ξ_t and ζ_t are, respectively, the x and y co-ordinates of target position, s_t is the target speed, θ_t is the target heading and $\omega_t \in \mathbb{R}$ is the turn rate. The target state is the solution of the Itô SDE

$$dx_t = f_p(x_t)\,dt + g_p\,d\beta_t, \qquad t > 0, \tag{1}$$

where $x_0 \sim \pi_0$, $\{\beta_t = (\beta_t^1, \beta_t^2)'\}$ with $\{\beta_t^1\}$ and $\{\beta_t^2\}$ mutually independent standard Wiener processes and

$$f_p(x_t) = (s_t \cos(\theta_t), s_t \sin(\theta_t), 0, \omega_t, 0)'$$
$$g_p = \begin{pmatrix} 0 & 0 & \sigma_s & 0 & 0 \\ 0 & 0 & 0 & 0 & \sigma_\omega \end{pmatrix}'$$

The process $\{\beta_t\}$ is assumed to be independent of x_0.

2.2. Cartesian velocty dynamic model

For the Cartesian velocity model, the target state $z_t = (\xi_t, \zeta_t, \dot{\xi}_t, \dot{\zeta}_t, \omega_t)'$ satisfies

$$dz_t = f_c(z_t)dt + g_c(z_t)d\beta_t, \qquad t > 0, \tag{2}$$

where $z_0 \sim \varpi_0$ is independent of $\{\beta_t\}$ and

$$f_c(z_t) = (\dot{\xi}_t, \dot{\zeta}_t, -\omega_t\dot{\zeta}_t, \omega_t\dot{\xi}_t, 0)'$$
$$g_c(z_t) = \begin{pmatrix} 0 & 0 & \sigma_s\dot{\xi}_t/s_t & \sigma_s\dot{\zeta}_t/s_t & 0 \\ 0 & 0 & 0 & 0 & \sigma_\omega \end{pmatrix}'.$$

with $s_t = \sqrt{\dot{\xi}_t^2 + \dot{\zeta}_t^2}$.

2.3. Measurement model

Measurements of the target position in polar co-ordinates are made at times $t_1, t_2, \ldots$ by a sensor located at the origin. For the polar velocity dynamic model, the measurement equation is

$$y_k = h(x_{t_k}) + e_k = \begin{pmatrix} \sqrt{\xi_{t_k}^2 + \zeta_{t_k}^2} \\ \arctan(\zeta_{t_k}/\xi_{t_k}) \end{pmatrix} + e_k \tag{3}$$

where $\{e_k \sim N(0, R)\}$ is white and independent of the initial state x_0 and the Wiener process $\{\beta_t\}$. The measurement equation for the Cartesian velocity dynamic model is similarly defined.

3. DISCRETISATION OF THE CT DYNAMIC MODEL

3.1. The Euler approximation

The Euler approximation is obtained by applying the Itô lemma [8] to the integral form of the SDE and retaining only single integral terms. The Euler approximation to the polar velocity dynamic model leads to the following stochastic difference equation for $t > \tau \geq 0$:

$$x_t = a_{p,1}(x_\tau) + G_{p,1}w_t \tag{4}$$

where $a_{p,1}(x_\tau) = x_\tau + (t-\tau)f_p(x_\tau)$, $G_{p,1} = \sqrt{t-\tau}\,g_p$ and $w_t \sim N(0, I_2)$ with I_m the $m \times m$ identity matrix.

The Euler approximation for the Cartesian velocity model is found in a simliar manner to give the following approximation:

$$z_t = a_{c,1}(z_\tau) + G_{c,1}(z_\tau)w_t \tag{5}$$

where $a_{c,1}(z_\tau) = z_\tau + (t-\tau)f_c(z_\tau)$, $G_{c,1}(z_\tau) = \sqrt{t-\tau}\,g_c(z_\tau)$ and $w_t \sim N(0, I_2)$.

The Euler approximation is an order 1 weak Taylor scheme [10]. This means that $\hat{x}_t$ generated according to (4) satisfies, with $\beta = 1$,

$$|\mathsf{E}\{g(x_t) - g(\hat{x}_t)\}| \leq C(t-\tau)^\beta \tag{6}$$

where $g : \mathbb{R}^{n_x} \to \mathbb{R}$ is a $2(\beta+1)$ times continuously differentiable function and C is a constant. An approximation which satisfies (6) with a larger value of β, therefore providing faster weak convergence, can be obtained by retaining more terms in the stochastic Taylor expansion.

3.2. An order 2 weak Taylor approximation

Higher order Taylor approximations to a SDE can be obtained by repeated application of the Itô lemma. The order 2 weak Taylor approximation to the SDE governing target motion for the polar velocity model can be found, after some working, as

$$x_t = a_{p,2}(x_\tau) + G_{p,2}(x_\tau)w_t \tag{7}$$

where, with $\delta = t - \tau$, $w_t \sim N(0, I_4)$ and

$$a_{p,2}(x_\tau) = \begin{pmatrix} \xi_\tau + \delta s_\tau \cos(\theta_\tau) - \delta^2 s_\tau\omega_\tau \sin(\theta_\tau)/2 \\ \zeta_\tau + \delta s_\tau \sin(\theta_\tau) + \delta^2 s_\tau\omega_\tau \cos(\theta_\tau)/2 \\ s_\tau \\ \theta_\tau + \delta\omega_\tau \\ \omega_\tau \end{pmatrix}$$
$$G_{p,2}(x_\tau) = E_p(x_\tau)V_\delta$$

with

$$E_p(x_\tau) = \begin{pmatrix} \sigma_s\cos(\theta_\tau) & 0 & 0 & 0 \\ \sigma_s\sin(\theta_\tau) & 0 & 0 & 0 \\ 0 & 0 & \sigma_s & 0 \\ 0 & \sigma_\omega & 0 & 0 \\ 0 & 0 & 0 & \sigma_\omega \end{pmatrix}$$
$$V_\delta = \begin{pmatrix} \sqrt{\delta^3/3} & 0 \\ \sqrt{3\delta}/2 & \sqrt{\delta}/2 \end{pmatrix} \otimes I_2$$

where $\otimes$ denotes the Kronecker product. Random variables generated according to (7) satisfy (6) with $\beta = 2$.

The weak order 2 Taylor approximation to the SDE governing the target motion for the Cartesian velocity model is

$$z_t = a_{c,2}(z_\tau) + G_{c,2}(z_\tau)w_t \tag{8}$$

where $w_t \sim N(0, I_4)$ and

$$a_{c,2}(z_\tau) = \begin{pmatrix} \xi_\tau + \delta\dot{\xi}_\tau - \delta^2\omega_\tau\dot{\zeta}_\tau/2 \\ \zeta_\tau + \delta\dot{\zeta}_\tau + \delta^2\omega_\tau\dot{\xi}_\tau/2 \\ \dot{\xi}_\tau - \delta\omega_\tau\dot{\zeta}_\tau - \delta^2\omega_\tau^2\dot{\xi}_\tau/2 \\ \dot{\zeta}_\tau + \delta\omega_\tau\dot{\xi}_\tau - \delta^2\omega_\tau^2\dot{\zeta}_\tau/2 \\ \omega_\tau \end{pmatrix}$$
$$G_{c,2}(z_\tau) = E_c(z_\tau)V_\delta$$

with

$$E_c(z_\tau) = \begin{pmatrix} \sigma_s\dot{\xi}_\tau/s_\tau & 0 & 0 & 0 \\ \sigma_s\dot{\zeta}_\tau/s_\tau & 0 & 0 & 0 \\ 0 & -\sigma_\omega\dot{\zeta}_\tau & \sigma_s(\dot{\xi}_\tau - \delta\omega_\tau\dot{\zeta}_\tau)/s_\tau & 0 \\ 0 & \sigma_\omega\dot{\xi}_\tau & \sigma_s(\dot{\zeta}_\tau + \delta\omega_\tau\dot{\xi}_\tau)/s_\tau & 0 \\ 0 & 0 & 0 & \sigma_\omega \end{pmatrix}$$

where $s_\tau = \sqrt{\dot{\xi}_\tau^2 + \dot{\zeta}_\tau^2}$.

The order 2 weak Taylor approximation will be referred to as the TS2 approximation.

4. PARTICLE FILTERING ALGORITHMS

In this section the discrete-time dynamic models derived in Section 3 are used to develop a particle filtering algorithm for CT target tracking. The algorithm will be developed using the state vector x_t for the polar velocity dynamic model although it is equally applicable to the Cartesian velocity model.

A particle filter represents the posterior distribution of the target state by random samples with associated weights. A common way of acquiring the random samples is via sequential importance sampling (SIS) [1]. In this paper a variant of SIS called the auxiliary particle filter [13] is used. The use of the auxiliary particle filter is motivated by the need to avoid particle duplication when performing resampling [12].

Assume that the posterior distribution of the target state at time t_k, $k \geq 0$ is represented by a set of particles $x_{t_k}^1, \ldots, x_{t_k}^n$ with weights $w_k^1, \ldots, w_k^n$. Using this particle set the posterior density at time $k+1$ can be approximated as

$$\hat{p}(x_{t_{k+1}}|y^{k+1}) \propto p(y_{k+1}|x_{t_{k+1}}) \sum_{i=1}^{n} w_k^i p(x_{t_{k+1}}|x_{t_k}^i) \qquad (9)$$

The PF seeks a sample from the mixture distribution (9) which can be interpreted as sampling from

$$\hat{p}(x_{t_{k+1}}, c|y^{k+1}) \propto p(y_{k+1}|x_{t_{k+1}}) p(x_{t_{k+1}}|x_{t_k}^c) w_k^c \qquad (10)$$

where $c \in \{1, \ldots, n\}$, referred to as the auxiliary variable, is an index on the mixture. The idea of the auxiliary particle filter is to sample from (10) using an importance density of the form

$$q(x_{t_{k+1}}, c|y^{k+1}) \propto p(y_{k+1}|\mu_{k+1}^c) p(x_{t_{k+1}}|x_{t_k}^c) w_k^c \qquad (11)$$

where μ_{k+1}^c is a quantity which characterises $p(x_{t_{k+1}}|x_{t_k}^c)$. For $i = 1, \ldots, n$, we select $c^i = l$ with probability proportional to $p(y_{k+1}|\mu_{k+1}^l) w_k^l$ and draw $x_{t_{k+1}}^i$ from $p(\cdot|x_{t_k}^{c^i})$. The weight update factor can be obtained, after dividing (10) by (11), as

$$p(y_{k+1}|x_{t_{k+1}}^i)/p(y_{k+1}|\mu_{k+1}^{c^i}), \qquad i = 1, \ldots, n. \qquad (12)$$

In the following we use $\mu_{k+1}^c \sim p(\cdot|x_{t_k}^c)$ and refer to the resulting algorithm as the auxiliary bootstrap filter (ABF). A draw from the transition density $p(x_{t_{k+1}}|x_{t_k})$ is approximated by splitting the sampling interval into m discretisation intervals and generating, for $l \in \{1, 2\}$,

$$x_{t_k+(j+1)T_k/m} = a_{p,l}(x_{t_k+jT_k/m}) + G_{p,l}(x_{t_k+jT_k/m}) w_{t_k,j}$$

for $j = 0, \ldots, m-1$ where $T_k = t_{k+1} - t_k$ and $w_{t_k,j} \sim N(0, I_{2l})$.

5. PERFORMANCE ANALYSIS

The analysis of this section will examine separately the Euler approximation vs. the TS2 approximation and the polar velocity model vs. the Cartesian velocity model.

The following scenario will be used. The initial state $x_0 \sim N(\mu_0, \Sigma_0)$ with

$$\mu_0 = (1000, 2650, 150, \pi/2, -\pi/45)'$$
$$\Sigma_0 = \text{diag}(400, 400, 25, (5\pi/180)^2, (0.2\pi/180)^2)$$

The driving noise parameters are $\sigma_s^2 = 1/5$ and $\sigma_\omega^2 = 5 \times 10^{-7}$. Target trajectories are generated according to (1) using the Euler approximation with $m = 1000$ intervals per sampling instant. The measurement noise covariance matrix is $R = \text{diag}(100, (\pi/180)^2)$. Measurements are collected for 120s with a constant sampling period. Error statistics are computed using 1000 realisations.

5.1. Euler approximation vs. TS2 approximation

In this set of simulations the ABF with the Euler and TS2 approximations is applied to the scenario described above. The polar velocity target dynamic model is used and the number of particles is set to $n = 2000$.

The statistic used here is the root mean square (RMS) error, i.e, the square root of the time averaged MSE. The RMS errors of the y-velocity $\dot{\zeta}_t$ and turn rate ω_t are plotted against the number m of discretisation intervals per sampling period in Figures 1 and 2 for sampling periods of $T = 2$s and $T = 5$s respectively. The main difference between the two discretisation techniques arises in the estimation of the target velocity. For accurate estimation of the y-velocity the TS2 approximation requires only a single discretisation interval per sampling period for both $T = 2$s and $T = 5$s while the Euler approximation requires $m = 4$ discretistion intervals for $T = 2$s and $m = 8$ discretistion intervals for $T = 5$s. Similiar results are obtained for the remaining elements of the state vector with the exception of the turn rate which is estimated accurately by both discretisation techniques even for $m = 1$.

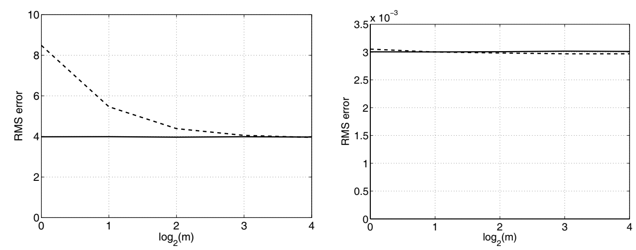

(a) (b)

Figure 1: RMS error plotted against the number of discretisation intervals per sampling period for the ABF-TS2 (solid) and ABF-E (dashed) using the polar velocity model. Results are shown for (a) $\dot{\zeta}_t$ and (b) ω_t. The sampling period is 2 seconds.

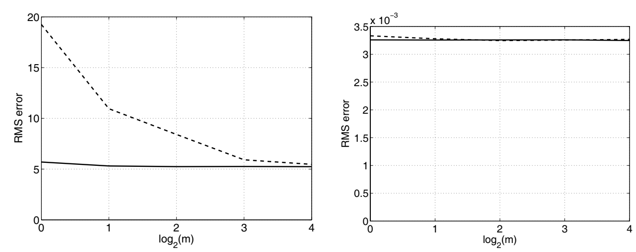

(a) (b)

Figure 2: RMS error plotted against the number of discretisation intervals per sampling period for the ABF-TS2 (solid) and ABF-E (dashed) using the polar velocity model. Results are shown for (a) $\dot{\zeta}_t$ and (b) ω_t. The sampling period is 5 seconds.

5.2. Polar velocity model vs. Cartesian velocity model

The comparison between the polar and Cartesian velocity dynamic models is performed with the TS2 approximations. The sample size for the ABF is 2000 and $m = 1$ discretisation interval per sampling period is used. Figure 3 shows the mean squared errors of the estimators of x-velocity and turn rate plotted on a log scale against time. The posterior Cramér-Rao bound (PCRB), derived using the method of [3], is also shown. Little difference can be discerned between the performances of the ABF-TS2 with polar and Cartesian velocity models. This can be attributed to the accuracy of the TS2 approximation which renders negligible any differences due to the form of the state vector. To demonstrate this the simulations are repeated with a sampling period of 5 seconds with the results shown in Figure 4. An appreciable difference between the performances of the two coordinate systems can be observed with the ABF-TS2 performing significantly better with the polar velocity dynamic model, particularly for estimation of the turn rate. This is in agreement with the results obtained in [7] using the extended Kalman filter with a simpler dynamic model.

A point of interest is the discrepancy between the accuracy of the position and velocity estimates and the PCRB. This discrepancy does not disappear even for larger numbers of particles. A possible explanation is the presence of "asymptotic biasedness" which has been shown to result in an optimistic PCRB for bearings-only tracking [4]. Asymptotic biasedness is a result of the finite range of the angle measurements.

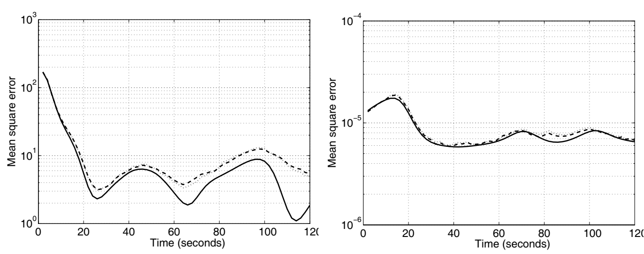

(a) (b)

Figure 3: Mean square error plotted against time for the ABF-TS2 using the polar velocity model (dashed) and Cartesian velocity model (dotted). Results are shown for (a) $\dot{\xi}_t$ and (b) ω_t. The sampling period is 2 seconds. The PCRB is shown as a solid line.

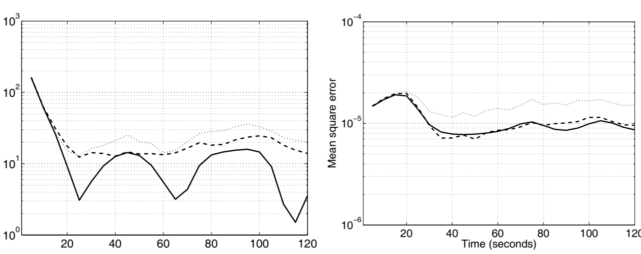

(a) (b)

Figure 4: Mean square error plotted against time for the ABF-TS2 using the polar velocity model (dashed) and Cartesian velocity model (dotted). Results are shown for (a) $\dot{\xi}_t$ and (b) ω_t. The sampling period is 5 seconds. The PCRB is shown as a solid line.

6. CONCLUSIONS

A new approach to coordinated turn tracking in which stochastic Taylor series expansions are used to provide discrete-time approximations to the target dynamics was developed. The form of the resulting stochastic difference equation describing the target motion does not permit exact solution of the tracking problem so a particle filtering algorithm, which is asymptotically exact, was proposed. A simulation analysis showed that a second order stochastic Taylor series expansion provides accurate discretisation and that better performance can be obtained by storing the target velocity in polar coordinates as opposed to Cartesian coordinates.

7. REFERENCES

[1] M. Arulampalam, S. Maskell, N. Gordon, and T. Clapp, "A tutorial on particle filters for online nonlinear/non-Gaussian Bayesian tracking," *IEEE Transactions on Signal Processing*, vol. 50, no. 2, pp. 174–188, 2002.

[2] Y. Bar-Shalom and X.-R. Li, *Estimation and Tracking: Principles, Techniques and Software*. Artech House, 1993.

[3] N. Bergman, "Posterior Cramér-Rao bounds for sequential estimation," in *Sequential Monte Carlo Methods in Practice*, A. Doucet, N. de Freitas, and N. Gordon, Eds. Springer, 2001, pp. 321–338.

[4] T. Brehard and J.-P. Le Cadre, "Initialization of particle filter and posterior Cramér-Rao bound for bearings-only tracking in modified polar coordinate system," *Submitted to IEEE Transactions on Aerospace and Electronic Systems*.

[5] P. Del Moral and J. Jacod, "Interacting particle filtering with discrete observations," in *Sequential Monte Carlo Methods in Practice*, A. Doucet, N. de Freitas, and N. Gordon, Eds. Springer, 2001, pp. 43–76.

[6] N. Gordon, D. Salmond, and A. Smith, "Novel approach to nonlinear/non-Gaussian Bayesian state estimation," *IEE Proceedings-F*, vol. 140, no. 2, pp. 107–113, 1993.

[7] F. Gustafsson and A. Isaksson, "Best choice of coordinate system for tracking coordinated turns," in *Proceedings of the IEEE Conference on Decision and Control*, Kobe, Japan, 1996, pp. 3145–3150.

[8] A. Jazwinski, *Stochastic Processes and Filtering Theory*. Academic Press, 1970.

[9] S. Julier, J. Uhlmann, and H. Durrant-Whyte, "A new method for the nonlinear transformation of means and covariances in filters and estimators," *IEEE Transactions on Automatic Control*, vol. 45, no. 3, pp. 477–482, 2000.

[10] P. Kloeden and E. Platen, *Numerical Solution of Stochastic Differential Equations*. Springer Verlag, 1992.

[11] D. Lerro and Y. Bar-Shalom, "Tracking with debiased consistent converted measurements versus EKF," *IEEE Transactions on Aerospace and Electronic Systems*, vol. 29, no. 3, pp. 1015–1022, 1993.

[12] M. Morelande and S. Challa, "Particle filtering algorithms for tracking manoeuvring targets in clutter from angle-only measurements," *IEEE Transactions on Aerospace and Electronic Systems*, (to appear).

[13] M. Pitt and N. Shephard, "Filtering via simulation: auxiliary particle filters," *Journal of the American Statistical Association*, vol. 94, pp. 590–599, 1999.